Transient Filamentation of a Laser Beam in a Thermal Force Dominated Plasma

A. K. Lal,[1] K. A. Marsh,[1] C. E. Clayton,[1] C. Joshi,[1] C. J. McKinstrie,[2] J. S. Li,[2] and T. W. Johnston[3]
[1]*Electrical Engineering Department, University of California, Los Angeles, California 90024*
[2]*Department of Mechanical Engineering, University of Rochester, Rochester, New York 14627 and Laboratory for Laser Energetics, 250 East River Rd.Rochester, New York 14623*
[3]*Institute National de la Recherche Scientifique - Energie, Quebec, Canada*
(Received 13 August 1996)

Experimental evidence for the transient phase of the filamentation instability of a laser beam in a thermal force dominated plasma is presented. When the laser beam is crossed with a weaker degenerate probe beam at a small angle, the interference of the two beams drives a thermally enhanced ion grating which during its transient phase acts to seed the filamentation/forward Brillouin instability. [S0031-9007(96)02241-7]

PACS numbers: 52.40.Nk, 52.35.Mw, 52.35.Nx

The nonlinear optics of plasmas is one of the most actively studied areas in plasma physics [1]. In particular, a voluminous amount of literature exists on parametric instabilities [2] of a single intense electromagnetic wave as it propagates through a plasma. Yet when multiple laser beams overlap in a plasma, the nature of these instabilities can be strongly modified and indeed new effects can become apparent [3]. In this Letter we present experimental evidence for one such effect: the transient phase of the filamentation instability [4,5] when two laser beams are crossed at a small angle [6] in a low temperature plasma [7]. The cross beam geometry allows one to see this effect unambiguously, whereas if a single laser beam is used, self-focusing of this beam as a whole may mask filamentation even though the two may be occurring simultaneously.

Of the many parametric instabilities that can occur in a laser excited plasma, the filamentation [4] and forward-stimulated Brillouin scattering (F-SBS) [8] instabilities are very closely related, since both involve ion gratings that are comparable in magnitude, orientation, and growth times. The wave vector matching diagram for the two processes is shown in Fig. 1 (inset). Here k_0 is the pump wave, k_+ and k_- are the scattered electromagnetic waves, and $k_\perp$ is the ion wave grating. In the steady state the ion wave gratings which filament the beam have a zero frequency, whereas in F-SBS the gratings are ion acoustic waves [$\omega_{ac} = k_\perp c_s$, $c_s = \sqrt{(ZT_e + \gamma T_i)/M}$ is the ion acoustic velocity] which frequency down-shift (Stokes) and up-shift (anti-Stokes) the scattered light by the ion acoustic frequency. If, as in our experiment, the ion acoustic damping rate ν is small compared to the ion acoustic frequency ω_{ac}, and the pump pulse duration is only a few ion acoustic periods, we expect to see the transient phase [9] of the filamentation/F-SBS instabilities. During this phase these two instabilities become experimentally indistinguishable from one another because the ion response to the filamentation instability has a transient at the ion acoustic frequency ω_{ac} [3]. In this case the scattered light also acquires an ion acoustic frequency shift ω_{ac}, which is normally associated with the F-SBS instability. The difference between the two instabilities becomes pronounced at larger $k_\perp$, where the filamentation growth rates in steady state rapidly go to negligible values, while the F-SBS, which continues as a resonant three wave process, can have a significant growth rate [8].

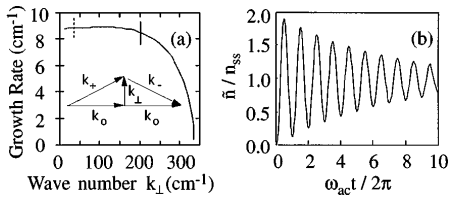

FIG. 1. (a) Steady-state filamentation growth rate as a function of wave number $k_\perp$. The dashed line at $k_\perp = 35$ corresponds to the k for whole beam self focusing, while the solid line at $k_\perp = 200$ is the location of the detectors. Inset shows the k-matching diagram for filamentation/forward-stimulated Brillouin scattering. (b) Solution of Eq. (4) for constant degenerate pump and probe beams, with $\nu/\omega_{ac} = 0.2$.

Although our work is in the transient regime, it is instructive to begin with the predictions of the steady-state theory. The steady-state spatial growth rate for the filamentation instability, obtained from perturbation theory, is shown in Fig. 1(a) and given by [10]

$$\Gamma = \frac{k_\perp}{2}\left\{2\frac{n_o}{n_c}[\gamma_p + \gamma_t(\kappa_{SH}/\kappa)] - \frac{k_\perp^2}{k_o^2}\right\}^{1/2} (\mathrm{cm}^{-1}), \quad (1)$$

with

$$\gamma_p = 9.33 \times 10^{-3}\frac{\lambda_o^2(\mu\mathrm{m})I(10^{14}\ \mathrm{W/cm^2})}{\sqrt{\epsilon}\,(1 + 1/Z)T(\mathrm{keV})}, \quad (2)$$

$$\gamma_t = 35.32\,\frac{I(10^{14}\ \mathrm{W/cm^2})Z^2(\ln\Lambda_b \ln\Lambda_c)}{T^5(\mathrm{keV})\sqrt{\epsilon}\lambda_o^2(\mu\mathrm{m})k_\perp^2}\,(n_o/n_c)^2. \quad (3)$$

Here γ_p is the ponderomotive contribution from the interference of the incident electromagnetic wave and the scattered waves, γ_t is the force due to localized heating, and $\kappa_{SH}/\kappa = 1 + (30k_\perp\lambda_e)^{4/3}$ is the reduction to the classical Spitzer-Harm conductivity due to nonlocal

 0031-9007/97/78(4)/670(4)$10.00

heat transport effects [11]. In the formula, I is the laser intensity in units of 10^{14} W/cm^2, λ_o is the laser wavelength in μm, T is the electron temperature in keV, n_o is the plasma density, n_c is the critical density, ϵ is the dielectric constant, $\ln\Lambda_b$ is the bremsstrahlung logarithm, $\ln\Lambda_c$ is the Coulomb logarithm, and λ_e is the electron delocalization length [11]. For Fig. 1(a), the following experimental and derived parameters were used: electron density $n_e = 9 \times 10^{16}$ cm^{-3} or 0.9% of critical density, electron temperature of 2.5 eV, peak laser intensity of 5×10^8 W/cm^2 at $\lambda_o = 10.6$ μm, $\lambda_e = 0.24$ μm, and a $Z \simeq 1$ nitrogen plasma with $m_i/m_p = 14$. Under these conditions, $\gamma_t \gg \gamma_p$ for $k_\perp = 2k_o \sin(\theta/2) \approx 200$ cm^{-1}, so the instability is driven primarily by the thermal force. In this figure the dotted line at perpendicular wave number $k_\perp = 35$ cm^{-1} indicates our wave number for whole beam self-focusing (WBSF). It is evident from Fig. 1(a) that if the laser beam contains sufficient power, WBSF will always accompany any filamentation growth.

When pump and probe beams cross in a plasma, the initial conditions can be significantly different. The temporal evolution of the normalized density modulation $\tilde{n}$ is now given by the equation [9]

$$\left(\frac{\partial^2}{\partial t^2} + 2\nu\frac{\partial}{\partial t} + \omega_{\rm ac}^2\right)\frac{\tilde{n}}{n_o} = -\frac{Z}{2}\frac{mc^2}{M}k_\perp^2(F_o^* F_+ + F_o F_-^*) \times (1 + A). \quad (4)$$

Here F_o, F_-, and F_+ are the normalized amplitudes $(v_{\rm osc}/c)$ of the pump and the scattered electromagnetic waves (k_- and k_+), respectively, $A = \gamma_t(\kappa_{\rm SH}/\kappa)/\gamma_p$ is the thermal enhancement factor, $v_{\rm osc}/c = eE/m\omega_o c$ is the normalized electron quiver velocity, m is the electron mass, M is the ion mass, and ω_o is the laser frequency. (The degenerate probe beam can be included in either the F_+ or F_-, depending on the direction at which it is injected.) The solution [12], subject to boundary conditions $\tilde{n}(0) = 0$ and $\partial\tilde{n}(0)/\partial t = 0$, assuming rapid onset of the drivers, and neglecting the evolution of the Stokes and anti-Stokes waves, is (for small $\nu/\omega_{\rm ac}$)

$$\tilde{n}(t) \propto [1 - e^{-\nu t}\cos(\omega_{\rm ac}t - \alpha)], \quad (5)$$

with $\alpha = \tan^{-1} = \nu/\omega_{\rm ac}$. Figure 1(b) depicts the response of such a harmonic oscillator to a constant driving force (with $\nu/\omega_{\rm ac} = 0.2$) due to degenerate pump and probe waves. The oscillator takes about one-half ion acoustic period to respond significantly. The transient response is larger than the steady-state response by a factor of $\sim$2 and takes several damping times to reach steady state. Since the ion acoustic period in our experiment is $\sim$40 ns, the collisional damping rate [13] is $\sim 0.2\omega_{\rm ac}$, and the laser pulse duration is only 150 ns, this transient is crucial in this experiment. The pump and probe beams now scatter from this density oscillation and produce Stokes and anti-Stokes waves in the direction of the probe beam and its mirror image (k_+ and k_-). The wave number mismatch for this to occur $\Delta k/k_\perp = c_s/c \approx 10^{-5}$ is much less than the angular spread in $k_\perp(10^{-2})$ due to the focusing optics. These waves, in turn, reinforce the grating which scatters even more frequency shifted light, thus completing the feedback loop for the forward-SBS instability. Because the ion grating with a well-defined $k_\perp$ is one dimensional and produces frequency shifted light, this response, which may be thought of as transient filamentation/F-SBS induced by the cross beam geometry, can be discerned even though WBSF and filamentation at other $k_\perp$ modes (which scatter light in two dimensions) may be simultaneously occurring.

The experimental setup is shown in Fig. 2(a). The arc discharge source [14] produces a large volume of singly ionized nitrogen plasma, whose axial and radial dimensions are approximately 1.5 cm. Over the laser spot size, there are no significant radial density or velocity gradients. The effect of axial flow on the nearly transverse ion wave is negligible. The plasma, which lasts for several microseconds, does not evolve over the time scale of the laser ($\sim$100 ns). The CO_2 laser is a TEA oscillator/amplifier system operating at 10.6 μm in a single longitudinal mode. The laser was operated at a peak intensity of $\sim 10^9$ W/cm^2 in a near diffraction limited 875 μm spot radius, with a rise time of $\sim$100 ns

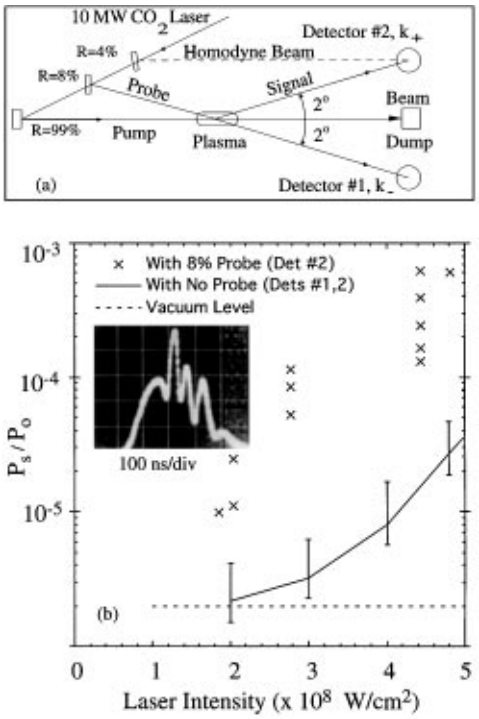

FIG. 2. (a) Experimental setup. An 8% probe beam intersects the pump at 2° in the plasma. Detectors 1 and 2 are placed symmetrically on both sides of the pump to measure the probe and signal beams. (b) Scattered power on detectors 1 and 2 as a function of pump laser intensity. The crosses show the signal on detector 2 when the probe beam is present. The solid line shows the signal without the probe beam, while the dashed line is the stray light level (without plasma or probe beam). The inset shows the scattered power as a function of time on detector 1, at $k_\perp = 200$ cm^{-1}, when a probe beam was present.

and a fall time of ~200 ns. The Rayleigh length (z_o = 23 cm) of these beams was much greater than the plasma size of ~1 cm. A beam splitter was used to divide the laser into the probe and pump beams with an intensity ratio $I_{pr}/I_o = 8\%$. The angle between the pump and probe beams (which were focused by the same optics) was about 1°. Two detectors (room temperature HgCdTe) were placed symmetrically about the pump beam to detect the scattered light in the direction of the probe beam, denoted by k_- (detector 1), and the signal beam, denoted by k_+ (detector 2), at an equal angle on the opposite side of the pump beam. In addition, a small fraction of the incident CO_2 beam could be used to bypass the plasma and mix with the scattered light (homodyning) on the detectors to detect any frequency shifts up to 0.5 GHz.

We have previously shown [14] that by adding a counterpropagating pump beam and measuring the properties of the phase conjugate signal that in this plasma, at $k_\perp = 400\ \mathrm{cm}^{-1}$, the thermal force contribution (which scales as $k_\perp^{-2}$) to the pump-probe grating is 16 times larger than the contribution of the ponderomotive force. Furthermore, by tuning the probe beam frequency we could resonantly enhance the phase conjugate signal when the pump and the probe beat at the ion acoustic frequency. From this we determined the value of c_s to be 8×10^5 cm/s [14]. The present filamentation experiments are carried out with a similar pump-probe geometry but with intensities a factor of 10 greater to exceed the thresholds for the self-focusing and F-SBS instabilities.

Now we discuss the experimental results. First, with the pump beam only, at a density of $9 \pm 2 \times 10^6\ \mathrm{cm}^{-3}$, we measured the scattered light as a function of pump intensity at detectors 1 and 2. This is shown as the solid line in Fig. 2(b). Up to an intensity of $2 \times 10^8\ \mathrm{W/cm}^2$, the amount of 10.6 μm light at detectors 1 and 2 when the pump beam traverses the plasma is about the same as the level of stray light from the pump beam through vacuum. Thereafter, the scattered light level increases exponentially with pump intensity. The duration of this signal is often shorter than that of the pump near the apparent threshold intensity of $2 \times 10^8\ \mathrm{W/cm}^2$. However, homodyning of this scattered signal with an external 10.6 μm signal on the detector showed no evidence of a low frequency modulation on the signal which might be characteristic of any ion acoustic shift. Furthermore, by reducing the pump signal to approximately $1 \times 10^8\ \mathrm{W/cm}^2$ (half the value needed for the onset of signal at these detectors) and adding a second counterpropagating beam containing the other half of the laser power (i.e., $1 \times 10^8\ \mathrm{W/cm}^2$), we could once again detect signal on detectors 1 and 2 [15]. It has been shown [16] that two counterpropagating beams, while stable individually, can become unstable in the presence of the other. For both the single and counterpropagating beam cases, the amount of signal on the two detectors increased exponentially with both plasma density and laser intensity. At higher powers, the scattered light on both detectors often showed modulations but not necessarily at any characteristic frequency. All of these observations are consistent with the signals on detectors 1 and 2 (solid line in Fig. 2) being due to whole beam self-focusing/filamentation of a whole spectrum of $k_\perp$ modes $[100 < k_\perp(\mathrm{cm}^{-1}) < 300]$ of the pump beam.

In order to see transient filamentation of a well-defined $k_\perp$, we kept the pump beam at $2 \times 10^8\ \mathrm{W/cm}^2$ and injected a probe beam at 2° ($k_\perp = 200\ \mathrm{cm}^{-1}$) containing approximately 8% of the pump power. The grating wavelength is approximately 300 μm, and there are about six grating periods across the focal diameter. At once we noticed that detector 1, which detected the probe beam exiting the plasma, had a sinusoidal modulation on it [Fig. 2(b), inset]. The frequency of this modulation was approximately the ion acoustic frequency, $\omega_{ac}/2\pi = 25 \pm 7$ MHz, using the previously measured value of c_s, and by doubling the angle between the pump and the probe beam, this frequency was doubled. As expected, when the pump and the probe beams were cross polarized, this modulation disappeared. The modulation observed is consistent with the probe beam, at frequency ω_o, mixing at the detector with the Stokes/anti-Stokes radiation at $\omega_o \pm \omega_{ac}$ that is generated when the pump scatters from the transient component of the ion wave to the density response given by Eq. (5).

The injection of the probe beam also produced a significant enhancement in the amount of scattered light on detector 2 (signal beam). In Fig. 2(b) the crosses show the signal when both the pump and probe beam are on. At $2 \times 10^8\ \mathrm{W/cm}^2$, the signal increases by a factor 5 (above the stray level) when the probe beam is present. If equal amounts of Stokes and anti-Stokes were present in this signal it would appear to be modulated at $2\omega_{ac}$. However, the signal does not appear modulated unless we mix it with a reference signal from the laser, upon which a similar frequency modulation as on detector 1 becomes evident, indicating that one of the two sidebands is preferentially excited. At $I_o = 1.8 \times 10^8\ \mathrm{W/cm}^2$ up to 3×10^{-5} of the pump power is converted into signal radiation in the k_+ direction compared to about 10^{-2} (deduced from the depth of modulation of the probe) in the k_- direction.

As the pump intensity is increased to approximately $4.5 \times 10^8\ \mathrm{W/cm}^2$, the amplitude of the signal beam increases from 3×10^{-5} up to $\sim 10^{-3}$ of the pump. Since the probe to pump power ratio is kept fixed at 8%, we might have expected a factor of 5 increase in the signal beam if optical mixing followed by Bragg scattering were responsible for enhancing the transient component of the density fluctuations $[\tilde{n}/n_o \sim I_o, P_{scat} \sim (\tilde{n}/n_o)^2]$. We are, therefore, definitely seeing exponentiation of an instability with roughly three *e*-foldings of growth from the initial noise level provided by optical mixing. A spatiotemporal model of filamentation [5,9] predicts the

Stokes wave to grow (for constant pumps) as

$$F_{-}(t) \propto \exp\left[1.5\left(\frac{1}{16}\frac{\omega_p^2}{\omega_o^2}\frac{c^2}{c_s^2}\frac{m}{M}F_o^2 GKt\right)^{1/3} - \nu t\right] \quad (6)$$

where $F_o = (v_{\rm osc}/c)$, $K = k_\perp^2 l^2$, $G = (\omega_{\rm ac}/2\nu)(1 + A)$ is the thermal enhancement term, and t is the time in acoustic periods. Since the laser in the experiment is not a constant step function, it has been approximated by using the average laser intensity and the FWHM of the pulse. This leads to a prediction of ~ 5 e-foldings of growth, in reasonable agreement with the experiment. At higher pump powers (5×10^8 W/cm^2) we have seen on detector 1 a modulation of the probe beam that is at $2\omega_{\rm ac}$ in addition to the modulation at $\omega_{\rm ac}$. This is shown in Figs. 3(a) and 3(b). This can only be due to having both Stokes and anti-Stokes components that are comparable in magnitude to the probe signal on the detector, further confirming that we are observing a nearly resonant, four wave instability [9].

In conclusion, we have observed the transient phase of the filamentation/forward-stimulated Brillouin instability. This is accomplished by intersecting two degenerate but unequal amplitude laser beams at a small angle in a plasma. The interference of the two beams drives a thermally enhanced ion grating which, during its transient phase, has a component at the ion acoustic frequency. This acts as an enhanced noise source from which the instability is seen to exponentiate. The transient response is clearly seen experimentally as amplitude modulation of the probe beam at approximately the ion acoustic frequency, and the generation of a signal beam that is also shifted in frequency by $\omega_{\rm ac}$, at a higher power level than what would be expected from optical mixing.

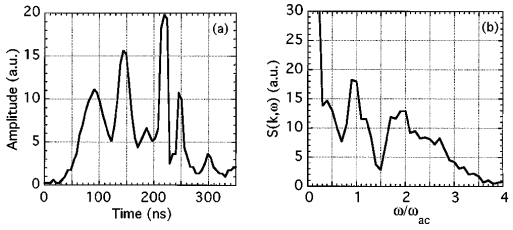

FIG. 3. (a) Scattered power vs time on detector 1 with a pump intensity of 5×10^8 W/cm^2 and a 8% probe beam. (b) FFT of this scattered power shows modulation at $2\omega_{\rm ac}$.

We thank Dr. W. B. Mori, Ritesh Narang, and Lorraine Ingraham for helpful discussions. This work was supported by U.S. DOE Grant No. DE-FG03-92ER40727 and the National Science Foundation under Contract No. PHY-9057093.

[1] *Advances in Plasma Physics*, edited by A. Simon and W. Thompson (Interscience Publishers, New York, 1976), Vol. 6.
[2] J. F. Drake *et al.*, Phys. Fluids **17**, 778 (1974); D. W. Forslund *et al.*, Phys. Fluids **18**, 1002 (1975).
[3] H. A. Rose and D. F. Dubois, Phys. Fluids B **4**, 252 (1992); G. G. Luther and C. J. McKinstrie, J. Opt. Soc. Am. B **9**, 1047 (1992); H. E. Huey *et al.*, Phys. Rev. Lett. **45**, 795 (1980); R. K. Kirkwood *et al.*, Phys. Rev. Lett. **76**, 2065 (1996).
[4] P. E. Young, Phys. Plasmas **2**, 2815 (1995); P. E. Young *et al.*, Phys. Rev. Lett. **63**, 2812 (1989); J. Limpouch *et al.*, Laser Part. Beams **6**, 295 (1988).
[5] H. Rose *et al.*, Sov. J. Plas. Phys. **16**, 537 (1990).
[6] W. L. Kruer *et al.*, Phys. Plas. **3**, 382 (1996); V. V. Eliseev *et al.*, Phys. Plas. **3**, 2215 (1996); C. J. McKinstrie *et al.*, Phys. Plas. **3**, 2686 (1996).
[7] M. S. Sodha *et al.*, Prog. Opt. **13**, 169 (1976).
[8] S. H. Batha *et al.*, Phys. Rev. Lett. **70**, 802 (1993); S. H. Batha *et al.*, Phys. Fluids B **5**, 2596 (1993).
[9] J. S. Li *et al.*, Bull. Am. Phys. Soc. **39**, 1584 (1994).
[10] E. M. Epperlein and R. W. Short, Phys. Fluids B **4**, 2213 (1992).
[11] E. M. Epperlein, Phys. Rev. Lett. **65**, 2145 (1990).
[12] M. Goldman and E. Williams, Phys. Fluids B **3**, 751 (1991).
[13] Y. Zhang and A. DeSilva, Phys. Rev. A **44**, 3841 (1991).
[14] Y. Kitagawa *et al.*, Phys. Rev. Lett. **62**, 151 (1989); A. Lal *et al.*, J. Opt. Soc. Am. B **8**, 2148 (1991).
[15] L. S. Ingraham *et al.*, Bull. Am. Phys. Soc. **39**, 1584 (1994); L. S. Ingraham, M.S. thesis, Thermal Self-focusing in Plasmas, UCLA (1994).
[16] G. G. Luther and C. J. McKinstrie, Phys. Rev. Lett. **68**, 1710 (1992).